C. R. Palevol 15 (2016) 393–406

Contents lists available at ScienceDirect

Comptes Rendus Palevol

www.sciencedirect.com

Human Palaeontology and Prehistory

Sedimentological study of major paleonto-archaeological localities of the Late Pliocene Quranwala zone, Siwalik Frontal Range, northwestern India

Étude sédimentologique des principales localités paléonto-archéologiques du Pliocène final de la zone Quranwala, chaîne frontale des Siwaliks, Nord-Ouest de l'Inde

Salah Abdessadok[a,*], Cécile Chapon Sao[a], Alina Tudryn[b], Anne Dambricourt Malassé[a], Mukesh Singh[c], Julien Gargani[b], Baldev Karir[c], Claire Gaillard[a], Anne-Marie Moigne[a], Vipnesh Bhardwaj[c], Surinder Pal[c]

[a] *HNHP, UMR 7194, Département de préhistoire, Histoire naturelle de l'Homme préhistorique, Muséum national d'histoire naturelle, Paris, France*
[b] *GEOPS, UMR 8148, Géosciences Paris-Sud, Université Paris-Sud, Orsay, France*
[c] *Society for Archaeological and Anthropological Research, Chandigarh, India*

ARTICLE INFO

Article history:
Received 16 February 2015
Accepted after revision 16 December 2015
Available online 3 February 2016

Handled by Anne Dambricourt Malassé

Keywords:
Siwalik Frontal Range
Late Pliocene
Masol Formation
Himalayan metamorphism
Sub-Himalayan floodplain
Fluvial deposits

ABSTRACT

Since 2008, the Indo-French research program 'Siwaliks' has been prospecting in the Late Pliocene formations of the Chandigarh anticline in the Northwest of India (Siwalik Frontal Range, Himalayan foothills). More than 200 quartzite tools and 1500 terrestrial vertebrate fossils have been collected from a Pliocene continental formation near the village of Masol. Several fossils show exceptional cut marks. A complete geological investigation of this area was performed in order to reconstruct the paleoenvironment. The geological sequences of the three major paleonto-archeological localities, Masol 1, Masol 6 and Masol 13, were studied. Silt and sandstone samples of the Quranwala fossiliferous area were collected to correlate the stratigraphy among the three localities and to understand the origins of the sediments. Three different techniques were used to analyze the sediments: a granulometric approach, X-ray diffraction and an analysis of heavy minerals. The sediment analysis demonstrates the relationship between the sample collected in Masol and the dismantling of the Higher as well as of the Lesser Himalaya. During the Late Pliocene, Masol was a floodplain with rich continental and freshwater fauna. The rivers were relatively calm, as indicated by the presence of apatite. Despite this, the quasi-simultaneous accumulations of quartzite cobbles and clay, as well as the presence of carcasses of small and large herbivores, suggest sudden climate variations probably due to the monsoon.

* Corresponding author. Département de préhistoire, Muséum national d'histoire naturelle, 1, rue René-Panhard, 75013 Paris, France.
E-mail address: abdess@mnhn.fr (S. Abdessadok).

http://dx.doi.org/10.1016/j.crpv.2015.09.020
1631-0683/

Mots clés :
Chaîne frontale des Siwaliks
Pliocène final
Formation Masol
Métamorphisme himalayen
Plaine sous-himalayenne
Dépôts fluviatiles

RÉSUMÉ

Depuis 2008, le programme de recherche franco-indien « Siwaliks » prospecte les formations du Pliocène tardif de l'anticlinal de Chandigarh, une petite chaîne du Nord-Ouest de l'Inde, qui s'intègre dans les piémonts de l'Himalaya (la chaîne frontale des Siwaliks). Plus de 200 outils en quartzite et 1500 fossiles de vertébrés d'eau douce et terrestres ont été collectés dans une boutonnière du Pliocène, autour du village de Masol. Quelques fossiles portent des traces exceptionnelles de découpe qui ont retenu l'attention, nécessitant une étude géologique complète de cette zone afin de reconstituer leur paléoenvironnement. Trois principales localités paléonto-archéologiques, Masol 1, Masol 6 et Masol 13, illustrent la séquence géologique de la zone fossilifère, dénommée *Quranwala zone*. Des échantillons de limons et de grès ont été prélevés afin de corréler la stratigraphie entre les trois localités et comprendre l'origine de leurs composants. La granulométrie, la détermination des minéraux argileux (aux rayons X) et des minéraux lourds (par microscopie) montrent qu'ils proviennent du démantèlement des haut et bas Himalaya, d'abord sous forme de blocs et de boues, avant d'être dispersés dans la plaine indo-gangétique qui borde les piémonts par des rivières dont la compétence diminuait vers l'aval. À la fin du Pliocène, Masol était une plaine d'inondation avec une riche faune d'eau douce et terrestre. Les rivières provenant des vallées de l'Himalaya étaient relativement calmes, comme l'indique la présence d'apatite. Néanmoins, les accumulations de galets de roches métamorphiques et de carcasses de petits et grands herbivores suggèrent également la présence de courants importants. Cette présence quasi simultanée de dynamiques fluviatiles énergétiques d'un côté et de conditions calmes de l'autre pourrait correspondre à des variations climatiques rapides attribuables à la mousson.

1. Introduction

Since 2008, an Indo-French program of research has conducted surveys in the hills around the village of Masol (northwestern India). The hills belong to the Siwalik Frontal Range close to the sub-Himalayan foothills (Fig. 1), and constitute a geological inlier (Badam, 1973; Gaur, 1987; Nanda, 1994; Patnaik, 2013), the exhumed oldest part of the Chandigarh anticline core (also called the Masol anticline). The exhumed rocks are rich in fossils known to belong to the Quranwala zone. The fossiliferous Quranwala zone (Sahni and Khan, 1968) is dated to the Late Pliocene (Ranga Rao et al., 1995; Ranga Rao, 1993; Chapon Sao et al., 2016a). From 2008 to 2015, the fieldwork covered an area of 50 hectares, and approximately 1500 vertebrate fossils were collected in 13 paleonto-archeological localities, named Masol 1, Masol 2 and so on, to Masol 13. The result was a collection of stone tools that were found on the surface (various choppers; Gaillard et al., 2016) and, for the first time, rare bones showing exceptional cut marks made by the sharp edge of quartzite cobble fragments (Dambricourt Malassé et al., 2016a,b). The faunal list includes a large number of herbivores, such as *Hexaprotodon* (Hippopotamidae), *Stegodon* (Proboscidean), several genera of bovids and cervids, *Sivatherium* (Giraffidae), rare carnivores (*Hyena*, *Panthera*) and also reptiles such as giant terrestrial turtles (*Colossochelys*) and crocodilians (*Crocodylus*) (Moigne et al., 2016). Very old butchering activity has been demonstrated at the Masol 1 and Masol 13 paleonto-archeological localities, and in the terrace of the Pichhli Choe (a *choe* is a small torrent).

The aim of this sedimentological study is the reconstruction of the paleo-environmental conditions during deposition of the sediments where fossils and stone tools were discovered. We identified clay and heavy minerals, and performed granulometry measurements on several samples. This study is a first approach to understanding the environmental context that prevailed during this period. More precisely this paper contributes to the sedimentological analysis of three major paleonto-archeological localities: Masol 1, Masol 6 and Masol 13.

2. Geological context

The Himalayan range is composed of three units: (i) the Higher Himalaya towards the Tibetan plateau, (ii) the Lesser Himalaya and (iii) the sub-Himalaya or foothills. The Higher Himalaya consists of metamorphic rocks of low and medium pressure (phyllites, quartzites, gneiss with kyanite, gneiss with porphyroblasts, gneiss with psammites, schists with kyanite) and magmatic rocks (granites with tourmaline and granites with biotite) (Singh et al., 2004). Minerals associated with plutonic rocks include blue tourmaline and zircon (Petitjohn, 1975), and minerals associated with metamorphic rocks include staurolite, kyanite, brown tourmaline, epidote and garnet (Singh et al., 2004). The Lesser Himalaya is constituted of metamorphic rocks with an increasing upward metamorphic grade (gneiss with biotite-garnet, schist with sillimanite and kyanite, marble) and intrusions of amphibolites, granites, pegmatites and presence of quartz (Jangpangi et al., 1978; Thakur et al., 1990). The metamorphic conditions allowed the presence (implementation) of the following minerals: hornblende, sillimanite, tourmaline, rutile and apatite (Jangpangi et al., 1978; Thakur et al., 1990).

The Siwalik Frontal Range is 2400 km long, extends from the Potwar Plateau (Pakistan) to North-East India (Assam), and constitutes the south-western border of Himalaya. Its

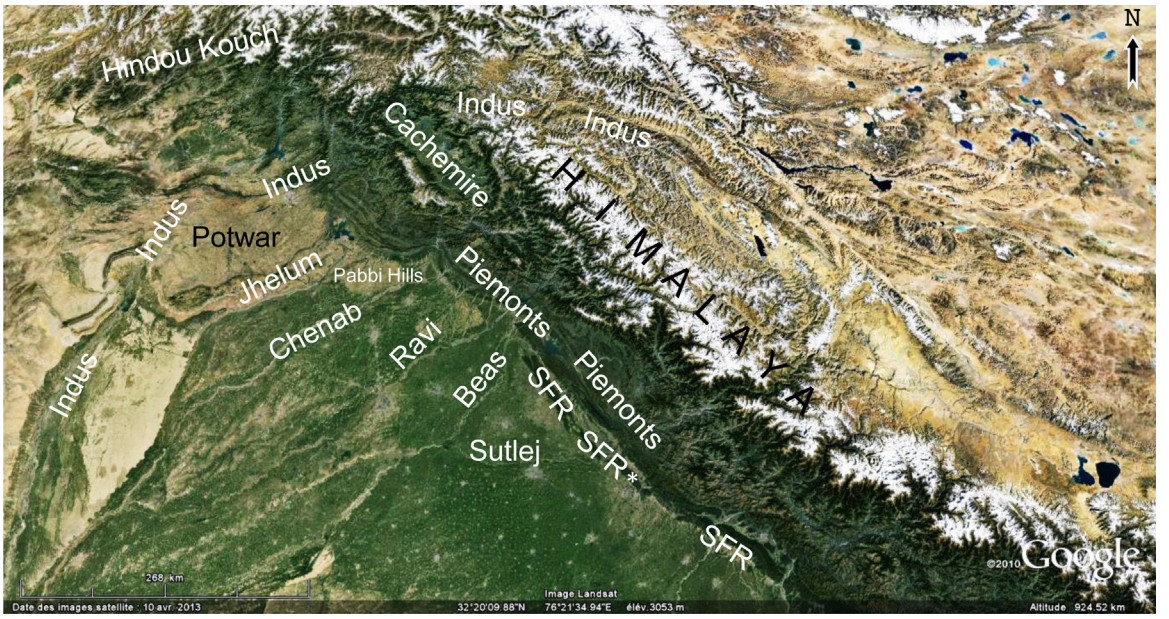

Fig. 1. View of the Northwest Indian subcontinent and the Upper Indus Basin, the rivers Jhelum, Chenab, Ravi and Sutlej. Star: the site of Masol in the Siwalik Frontal Range, map data ©Google 2015.
Fig. 1. Vue sur le Nord-Ouest du sous-continent Indien et le bassin supérieur de l'Indus, avec les rivières Jhelum, Chenab, Ravi et Sutlej. Étoile : le site de Masol dans la chaîne frontale des Siwaliks, données de carte ©Google 2015.

width varies from 10 to 50 km (Fig. 1). The geological formations are constituted of molasses formed during the dismantling of the Himalayan range. These molasses are divided into three subgroups: the Lower Siwalik (18 to 11.2 Ma), the Middle Siwalik (11.2 to 3.5 Ma) and the Upper Siwalik (3.5 Ma to 600 ka) (Warwick, 2007). The Upper Siwalik is divided into three faunal formations: Tatrot (Upper Pliocene), Pinjor (Lower and Middle Pleistocene) and the Boulder Conglomerate (Middle Pleistocene). The Chandigarh anticline corresponds mainly to the Pinjor and the Boulder Conglomerate. The Tatrot Formation is seen locally, as in Masol, and its upper part corresponds to the Quranwala zone (Fig. 2).

The study of heavy minerals from the Kumaun region (Uttarakhand, Higher Himalaya, northeast to Chandigarh anticline) (Tandon, 1972), suggests that staurolite and kyanite are markers of, respectively, the Lower and the Middle Siwalik. The same assemblage is found in Jammu (Northwest Himalaya) and the Punjab (foothills) regions with successive appearances of staurolite and kyanite, and

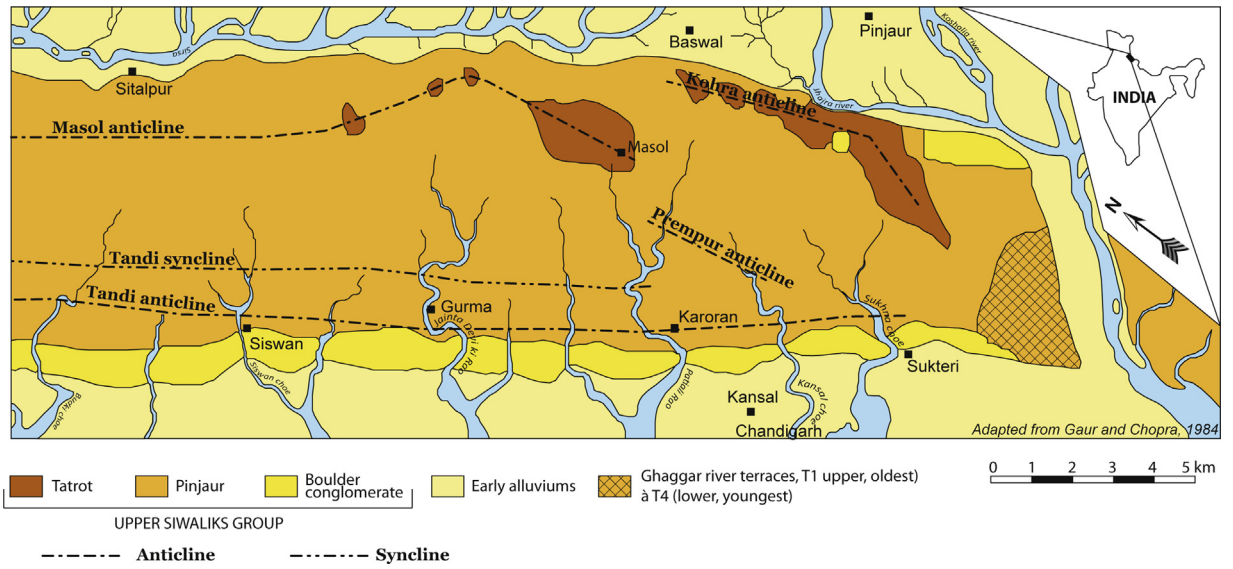

Fig. 2. Structural map of the Masol anticline, Siwalik Frontal Range, Punjab, NW India (Abdessadok, according to Sahni and Khan, 1968).
Fig. 2. Carte structurale de l'anticlinal de Masol, chaîne frontale des Siwaliks, Pendjab, Nord-Ouest de l'Inde (Abdessadok, d'après Sahni et Khan, 1968).

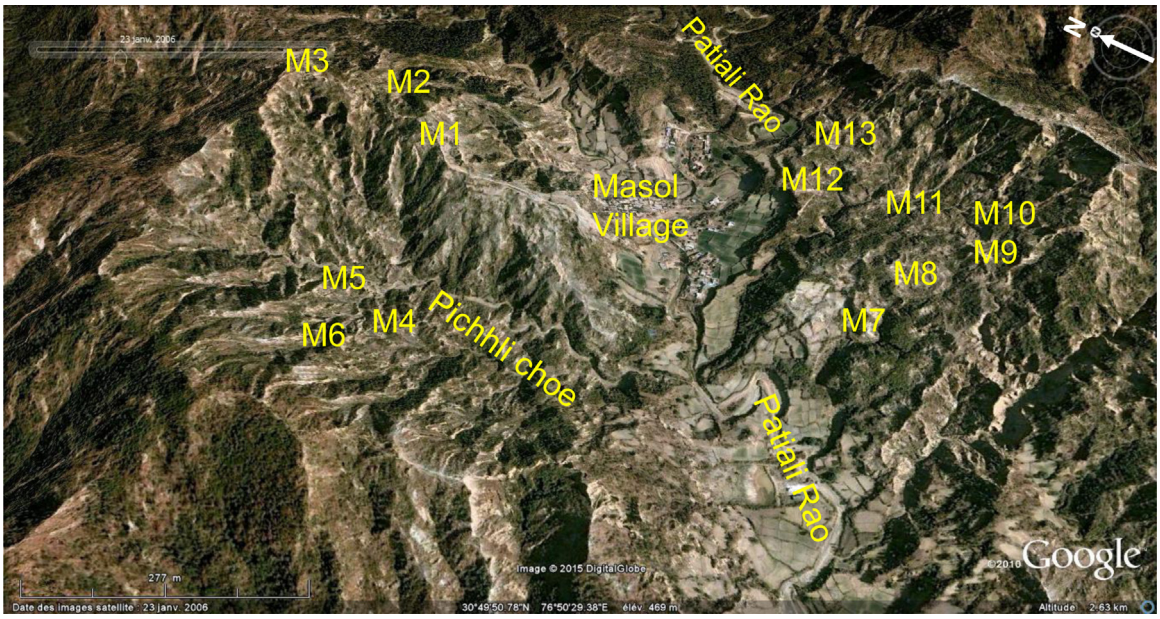

Fig. 3. View on Masol with the paleonto-archeological localities (1 to 13), Masol village, the Patiali Rao River and the Pichhli Choe watershed, map data ©Google2015).
Fig. 3. Vue générale sur Masol, avec les localités paléonto-archéologiques (1 à 13), le village de Masol, la rivière Patiali Rao et le bassin versant du Picchli Choe, données de carte ©Google 2015.

finally hornblende and sillimanite in the Lower, Middle and Upper Siwalik (Raju and Dehadrai, 1962; Singh et al., 2004). The minerals arise from metamorphic and magmatic rocks composed of gneiss, quartzite and granites. Based on the mineral markers, Singh et al. (2004) identified the origin of the sediments: staurolite and kyanite are transported from the Higher Himalaya, and sillimanite and hornblende are transported from the Lesser Himalaya.

The chronological appearances of different minerals in the Siwalik subgroups are related to the evolution of the Himalayan range. The mineral compositions correlate to the progressive erosion of the Himalayas contemporaneously with the Tibetan Plateau uplift: the staurolite in the Lower Siwalik, the kyanite in the Middle Siwalik (both of the two minerals are originated from Higher Himalaya) and then the sillimanite and hornblende (originating from Higher Himalaya) in the Upper Siwalik (DeCelles et al., 1998). Based on the chronology of Warwick (2007), the oldest erosion began in the formation of Higher Himalaya, which was rich in staurolite during latest Early Miocene (Lower Siwalik), and then affected the rocks of Higher Himalaya containing kyanite during the Late Miocene and the Early Pliocene (Middle Siwalik). The metamorphic formations of Lesser Himalaya with a high content of sillimanite and hornblende were later eroded during the Upper Pliocene and the Early Pleistocene (Upper Siwalik).

In the Chandigarh anticline (Upper Siwalik), the inlier of Masol is organized along two major axes. The main axis is constituted of the Masol anticline, oriented NW–SE and a seasonal river, the Patiali Rao which is the minor axis NE–SW, from the northern limit of the anticline towards the Indo-Gangetic plain at the southwest, cutting the anticline at the Masol village (Fig. 3). In the inlier, the vegetation is rather sparse, and comprised of bushes. The northwestern flank of the Patiali Rao is mainly made up of a long, high plateau. This plateau is bordered on its western side by the small watershed of a seasonal torrent, the Pichhli Choe, a tributary of the Patiali Rao. This choe eroded the Masol anticline and unearthed the fossiliferous Quranwala zone. On the south-east flank, the anticline is particularly eroded. The relief is a large plateau incised by ravines and small torrents.

The sedimentary sequence found at Masol is an alternation of sandstones and silt ~170 meters thick (Fig. 4). The magneto-stratigraphy all along the Patiali Rao (Ranga Rao, 1993; Ranga Rao et al., 1995) localizes the Gauss/Matuyama paleomagnetic reversal (2.588 Ma) at the end of the Quranwala zone sequence. Three main factors have shaped the Masol area: 1) the tectonics between the Indian and Asian plates with a folding of the floodplain around 600–400 ka, 2) the monsoon, and 3) the weak mechanical resistance of the sediments (Gargani et al., 2016).

Paleonto-archeological localities have been found on the two river flanks of Pichhli Choe (i.e. Masol 1 to Masol 6 on the western side, and Masol 7 to Masol 13 on the eastern side). Chapon Sao et al. (2016b) and Tudryn at al. (2016) established the log of the Masol area. They also established the stratigraphic position of all the paleonto-archeological localities in the sedimentary sequence, which is roughly compounded (made up) of silts/clay ("c") and sandstones ("s") numbered from 1 to 17 (for details see Tudryn et al., 2016) (Fig. 4). Three localities revealed hominin butchery activities (Dambricourt Malassé, 2016; Dambricourt Malassé et al., 2016a,b): a) Masol 1, b) the lower terrace of the Pichhli Choe below Masol 6 locality, and c) Masol 13. The Masol 1 and Masol 2 paleonto-archeological areas start from the same basal layers: the c3 silt and s3–s4 sandstones. Masol 6 corresponds to the c5 silt and s5 sand-

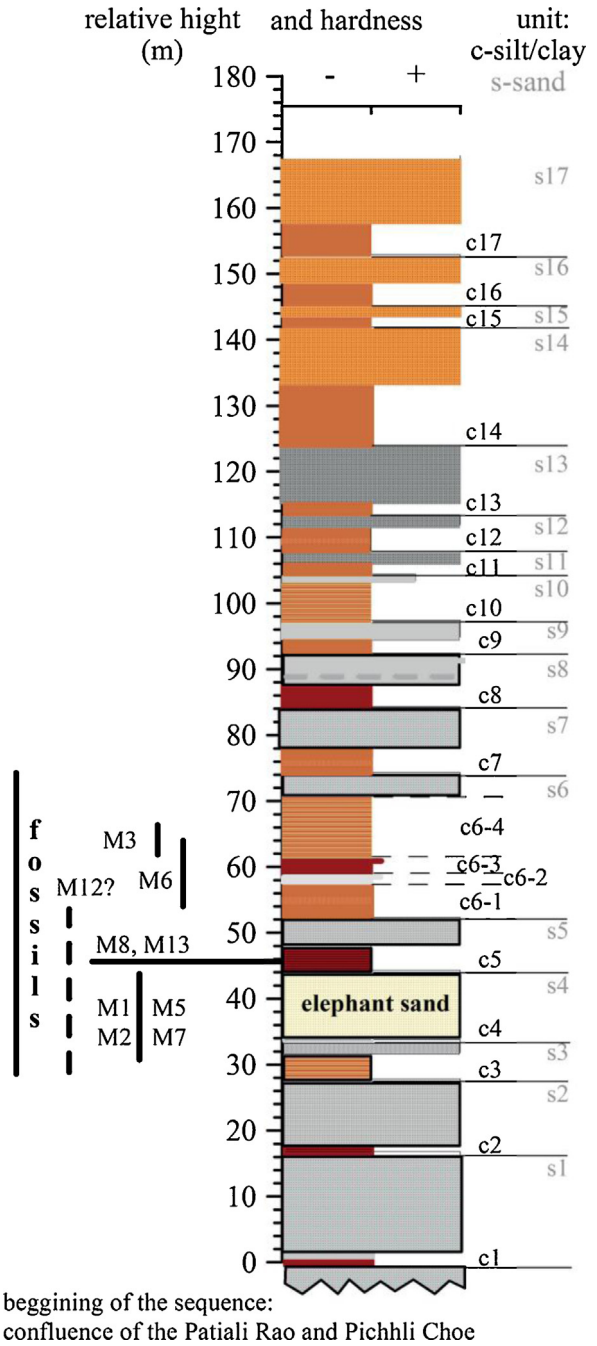

Fig. 4. General stratigraphic log.
Fig. 4. Log stratigraphique général.

stone. The Masol 13 locality contains the s4 sandstone, the c5 silt and dismantled s5 sandstones (Fig. 4; Chapon Sao et al., 2016b; Tudryn et al., 2016).

3. Fieldwork and methodology

Here we describe more accurately the mineralogical content of the sediments from three paleonto-archeological localities, Masol 1, Masol 6 and Masol 13 (Fig. 5), due to their significant paleoanthropological interest.

Each of the three sedimentary sequences from the paleonto-archeological localities detailed in this study are described from the bottom to the top, and following their stratigraphic order: Masol 1, Masol 13 and Masol 6. All the sequence consists of an alternation of silt and sandstones, which are described and called "members". Macroscopic description of sandy fractions made during the fieldwork demonstrates fine, medium and coarse grain sizes.

3.1. Fieldwork

Masol 1 paleonto-archeological locality

Masol 1 is located on the dome and on its western slopes (Fig. 3; Chapon Sao et al., 2016a; Gargani et al., 2016). The eponymous locality is the center of the anticline and is of significant interest as a result of cut marks found here on a fossil shaft tibia (Dambricourt Malassé et al., 2016a,b). Six sediment samples were collected at the site for the sedimentology and the paleomagnetic measurements (Chapon Sao et al., 2016b), 3 samples were collected in the silt and 3 others taken from the sandstones (Fig. 5).

- Member *F* is a light gray sandy silt ~2.40 meters thick. It is very compact, contains centimetric rock debris and white micas, and laminations are visible. One sample was taken here (S1).
- Members *E and D* represent a silty formation approximately 3 meters thick. The base of red wine color (1.80 m thick, Member D) is underlaid by an orange colored sediment (1.20 m thick, Member E). These sediments are very hard and contain pluricentrimetric polyhedral rock debris. There is no lamination. The presence of few hydromorphic forms (1–10 cm large) could be seen. There are no lateral variations. Two samples were collected in the red wine color silt (S2 and S3)
- Member *C* (Fig. 5): is approximately 1.20 meters thick. The base (10 cm thick) constitutes a very cohesive light gray silt that gradually changes towards the top into a light gray, fine grained, micaceous sandstone. No laminations are visible. One sample was taken from the micaceous fine sandstone (S4).
- member *B* (Fig. 5): is approximately 2.50 meters thick sequence of mainly medium to coarse sandstones. Several discontinuous cross-bedded levels of clay and gravels are visible. Two samples were taken (S5 and S6).

Masol 13 paleonto-archeological locality

Masol 13 is located on the eastern bank of the Patiali Rao River (Fig. 3) and like Masol 1, is of a significant interest due to the presence of cut marks on a bony splinter (Dambricourt Malassé et al., 2016b). The stratigraphic section is oriented east-west. Five samples were collected from four layers (Fig. 5). This locality contains, respectively from the bottom to the top:

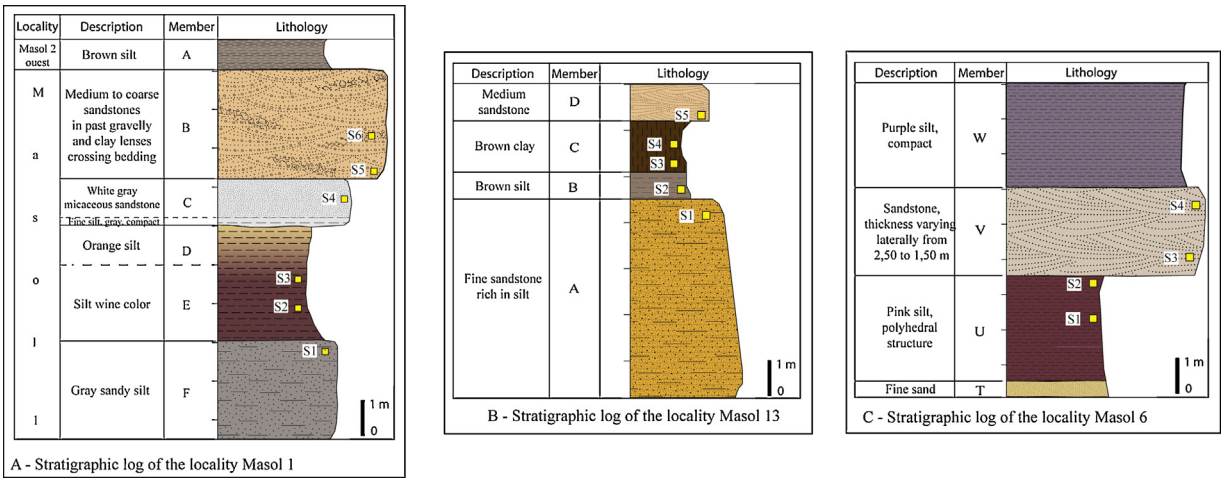

Fig. 5. Stratigraphic logs of the sections drawn in three localities of Masol. A: Masol 1; B: Masol 13; C: Masol 6 (Chapon Sao).
Fig. 5. Logs stratigraphiques des coupes relevées dans les trois localités de Masol. A : Masol 1 ; B : Masol 13 ; C : Masol 6 (Chapon Sao).

- Member *A:* Fine, light brown colored sandstone, 3 to 4.50 meters thick and containing silt. One sample was collected at the top of the layer (S1, Fig. 5).
- Member *B:* Brown, no laminated silt, 60 cm thick. One sample was collected (S2).
- Member *C:* Brown clay with some hydromorphic gray-green morphologies, and without lamination, 1.10 meter thick. Two samples were collected (S4 and S3).
- Member *D:* Gray medium sandstone, 80 cm thick, and without any sedimentary structures. The weathering of this layer seems to produce spheroidal blocks. One sample was collected (S5).

Masol 6 paleonto-archeological locality

Masol 6 is a large area located on the western flank of the Picchli Choe torrent, ~380 meters from Masol 1 (Fig. 3). This sector is the second richest locality in fossils and stone tools after Masol 1, with numerous accumulations of cobbles, sometimes in dismantled conglomerates on the slopes (Gaillard et al., 2016; Moigne et al., 2016) (Fig. 6). Until now the locality has not provided cut marks, but the area is above the bed of the Pichhli Choe and at 190 meters from its terrace T2 (Gargani et al., 2016) where a third bone with cut marks was collected (Dambricourt Malassé et al., 2016b).

The sampling was performed on a cliff divided into four members from the bottom to the top, T, U, V and W (Fig. 5) as follows:

- Member *T*: Yellow fine sandstone, friable, 0,46 meter thick (no sample).
- Member *U*: Pink silt, 3 meters thick, with a polyhedral structure (samples S1 and S2).
- Member *V*: Gray sandstone with lateral variation in thickness (2.50 to 1.50 meters thick) (samples S3 and S4).
- Member *W*: Silt of a purplish color and a compact structure, 3 meters thick (no sample).

3.2. Methodology

The samples were studied in France at the National Museum of Natural History, Paris, in the Laboratory of Sedimentology, at the Department of Prehistory, Institute of Human Paleontology (IPH) and in the Department of Earth History. Materials with a grain size < 2 mm were analyzed using two main approaches: (1) grain size measurement and, (2) sand and clay mineralogical analysis. A mass of 100 grams of material was required to carry out the various sedimentological analyses for each sample. The samples were dried at a temperature of 40 °C, and then the sediment was separated into grains sized below 2 mm (gravels) and above 2 mm (sand).

The grain size (coarse sand (2–0.2 mm), fine sand (0.2–0.040 mm), silt (0.040 mm–0.002 mm) and clay (< 0.002 mm)) was measured using a Malvern Mastersizer 2000 laser granulometer which performed diffraction and scattering measurements. The study was carried out using distilled water for the silty samples and without water for the sandy samples. Obscuration varied between 10 and 20 units. The interpretations were made according to the classical works of Anderson (2007), Folk and Ward (1957), Miskovsky and Debard (2002), Pye and Blott (2004) and Rivière (1977).

For **heavy minerals,** the works of Duplaix (1958), Parfenoff et al. (1970) and Tourenq (2002) were consulted. The sample was first sieved from 2 to 0.040 mm in order to retain only the sand fraction. This was attacked by hydrogen peroxide to remove organic matter and the decalcified with hydrochloric acid. The samples were then washed, several times, with distilled water and dried in an oven at 40 °C. The separation of heavy minerals was performed using a bromoform density equal to 2.89. For each sample, 250 to 300 grains were studied under a petrological microscope to determine the species.

For **the clay mineralogy**, we applied the method developed by Holtzapffel (1985). This consists of removing from

Fig. 6. Cobbles in fragmented conglomerate at Masol 6.
Fig. 6. Galets dans des fragments de conglomérat à Masol 6.

the sample, by chemical treatments, organic matter and carbonates, in order to deflocculate the clay. The fraction below 2 microns, which corresponds to clay, is extracted from the solution after a rest period of 1 hour 35 minutes. This mode of treatment allows oriented aggregates to be obtained. For each sample, three slides are prepared for three types of analysis: (1) aggregate N: without treatment, (2) aggregate G: sample exposed, during 24 hours, to the ethylene glycol vapor, and (3) aggregate CH: heated sample at 490 °C during 2 hours.

Analyses to determine the minerals from their crystallographic properties were conducted at the Department of Earth History. X-ray diffraction was performed on orientated aggregates using a diffractometer Bruker D2 Phaser Lynxeye (30 kV, 10 mA) with a Cu anti-cathode. A continuous scan from 3 to 65° was performed each 0.02° during 0.2 seconds for each step and the rotation speed was of 20 revolutions/min (0 to 80). The identification of crystalline phases was made using the software DIFFRAC.SUITE. For the determination of the clay minerals, the following works were consulted: Caillère et al. (1982), Larqué (2002), Millot (1964), Pédro (1965), Larqué (2002) and Robert (1975).

4. Results

4.1. Granulometry

Masol 1 paleonto-archeological locality

The silty-sand member "F" at the base of this sequence (Fig. 7) contains 52% silt and 48% sand. The two samples (S2 and S3) collected from silty layers "member E", contain 4% clay, 50% silt and 46% sand for sample S2, and 6% clay, 54% silt, 38% sand and 2% coarse sand for sample S3 (Fig. 7). The last three samples were collected in the micaceous sandstone (S4, member C; Fig. 5) and in the medium to coarse sandstones (S5 and S6, member B; Fig. 5). The three samples recorded a high rate of coarse sand (between 21 and 53%). Fine sand was also well represented (between 34 and 50%) and the silt decreased relative to the lower levels (13–30%) (Fig. 7).

Masol 13 paleonto-archeological locality

The S1 sample collected at the base of the section in a fine sandstone "Member A" is essentially constituted of fine sand (60%) and silt (27%), but also of coarse sand (9%) and clay (3%) (Fig. 7). Samples collected in the brown silt "member B" (S2) and brown clay "member C" (S3 and S4) as described during the field work, have the same low contents of clay (9%) and of coarse sand (1%) (Fig. 7). The percentages of silt and fine sand in S2 and S3 are identical (respectively 65% and 25%) (Fig. 7). In sample S4 (Fig. 7), silt abundance reaches 84%. The last sample (S5) collected in the sandstone at the top of the section (Member D) (Fig. 7) presents 49% fine sand and 39% silt, and there is an increase recorded in coarse sand (8%) and a decrease of clay (5%) compared to the S2, S3 and S4 samples.

Masol 6 paleonto-archeological locality

The first two samples (S1 and S2) collected in the pink silt "Member U" show completely different contents (Fig. 7). The S1 sample is very rich in silt (86%) and contains a large amount of clay (10%). Sample S2 contains a significant amount of sand (50% fine sand and 24% coarse sand) and a non-negligible amount of silt (26%). The two other samples (S3 and S4) collected in sandstone "Member V" contain identical proportions of fine sand (56%), silt (33%), coarse sand (7%) and clay (4%) (Fig. 7).

4.2. Clay minerals

The X-ray diffraction (XRD) measurements were taken on clay fraction of the sediment using three protocols: (1) classical for diffraction, (2) with samples heated at 490 °C, and (3) with samples treated with ethylene glycol. This allows the identification of illite, chlorite, kaolinite and smectite through the observation of four main peaks in the XRD spectrum.

A peak can be seen at 10 Å (Fig. 8). If the peak shows constant intensity whatever the treatment used, it is due to the presence of illite. A second peak is seen at 14 Å and is due to the chlorite, when the thickness of the peak is constant for all three protocols used (Holtzapffel, 1985). The two peaks at 7.2 Å (for the main peak) and 3.58 Å

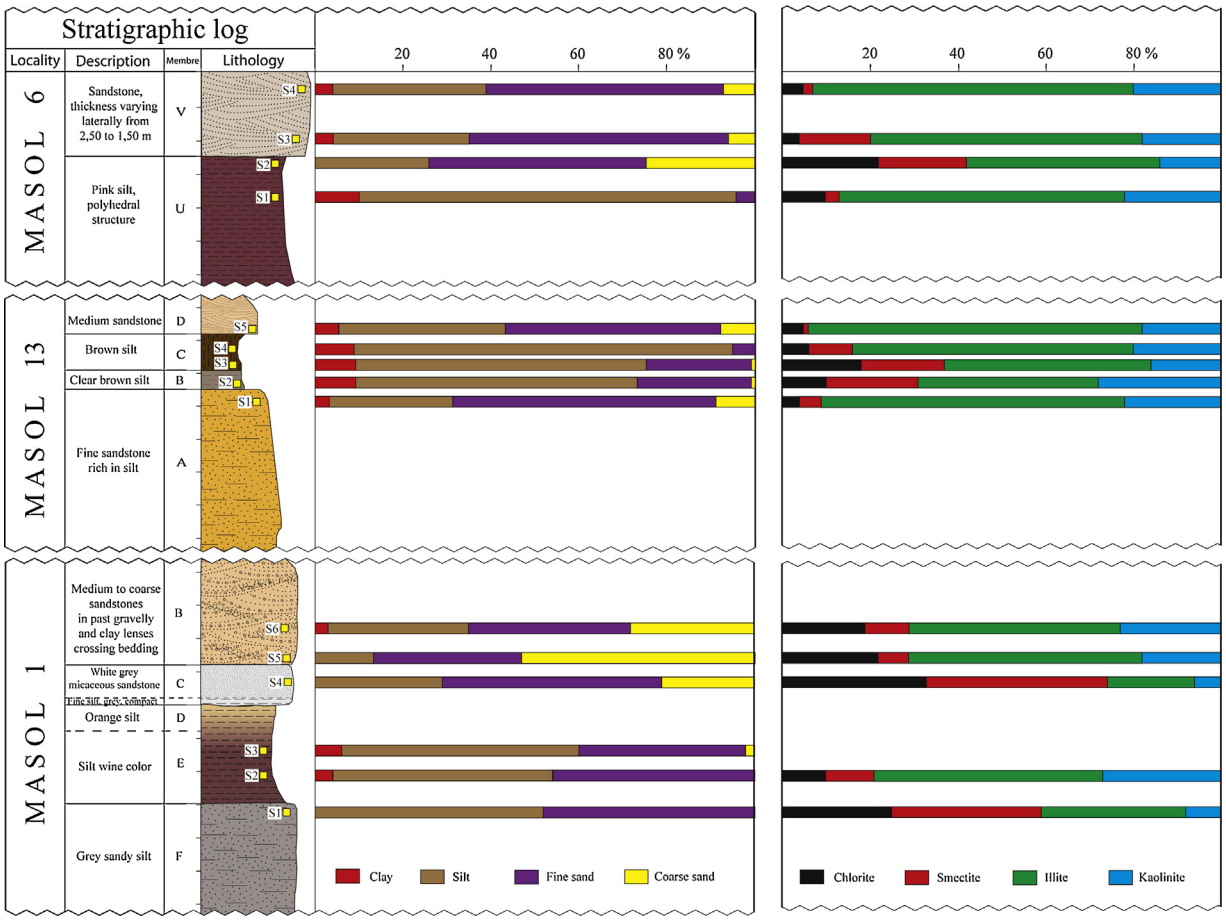

Fig. 7. Diagram of the particle size (left) and clay minerals (right) of the localities of Masol 1, Masol 13 and Masol 6.
Fig. 7. Diagramme des résultats granulométriques (à gauche) et des minéraux argileux (à droite) des localités Masol 1, Masol 13 et Masol 6.

(for the secondary peak), which disappear after heating at 490 °C, indicate the presence of kaolinite (Fig. 8). The peak at 14 Å (protocol without treatment), at 10 Å after heating at 490 °C and moving to 17 Å after its exposure to ethylene glycol, is characteristic of smectite (Lucas et al., 1959).

We first demonstrated the results in stratigraphic sections before synthesizing the characteristics of each locality.

Masol 1 paleonto-archeological locality

The illite content ranges between 48% and 53% in all the samples except for the micaceous fine sandstone, Sample S4, where it presents 20%. Its peak is long and narrow in almost all the samples (Fig. 8). This is a characteristic of a good crystalline network. In Sample S4, there is a significant quantity of smectite (41%) and of chlorite (33%). The kaolinite abundance ranges between 18 and 27% except in two samples (S4 and S1 with 6 and 8%, respectively). The smectite content ranges between 10 and 41%, and the chlorite content ranges between 10 and 33%.

Masol 13

The Masol 13 deposits are mainly characterized by the predominance of illite (41–76%). The well-defined peak of illite suggests a well-developed crystalline network (Caillère et al., 1982). The chlorite and the smectite are poorly represented in Samples S5, S4 and S1 (contents between 1 and 6%) but are significantly represented in Samples S2 and S3 (contents between 18 and 21%). Their peaks often take the form of domes in the spectrum, indicating the beginning of degradation of the crystal lattice (Dunoyer de Segonzac et al., 1968). The kaolinite abundance is constant and it is present in a significant proportion (between 16% and 22%) (Fig. 8).

Masol 6

The illite content ranges between 43 and 73% in all samples, the kaolinite between 14 and 22% (Fig. 8). The chlorite abundance ranges between 4 and 10% and the smectite abundance between 2 and 20%.

Clay mineral synthesis

The illite is very abundant in all the silty layers of the three localities, and is scarce in the micaceous fine sandstone (member C) of Masol 1. Smectite and chlorite are present mainly at Masol 1.

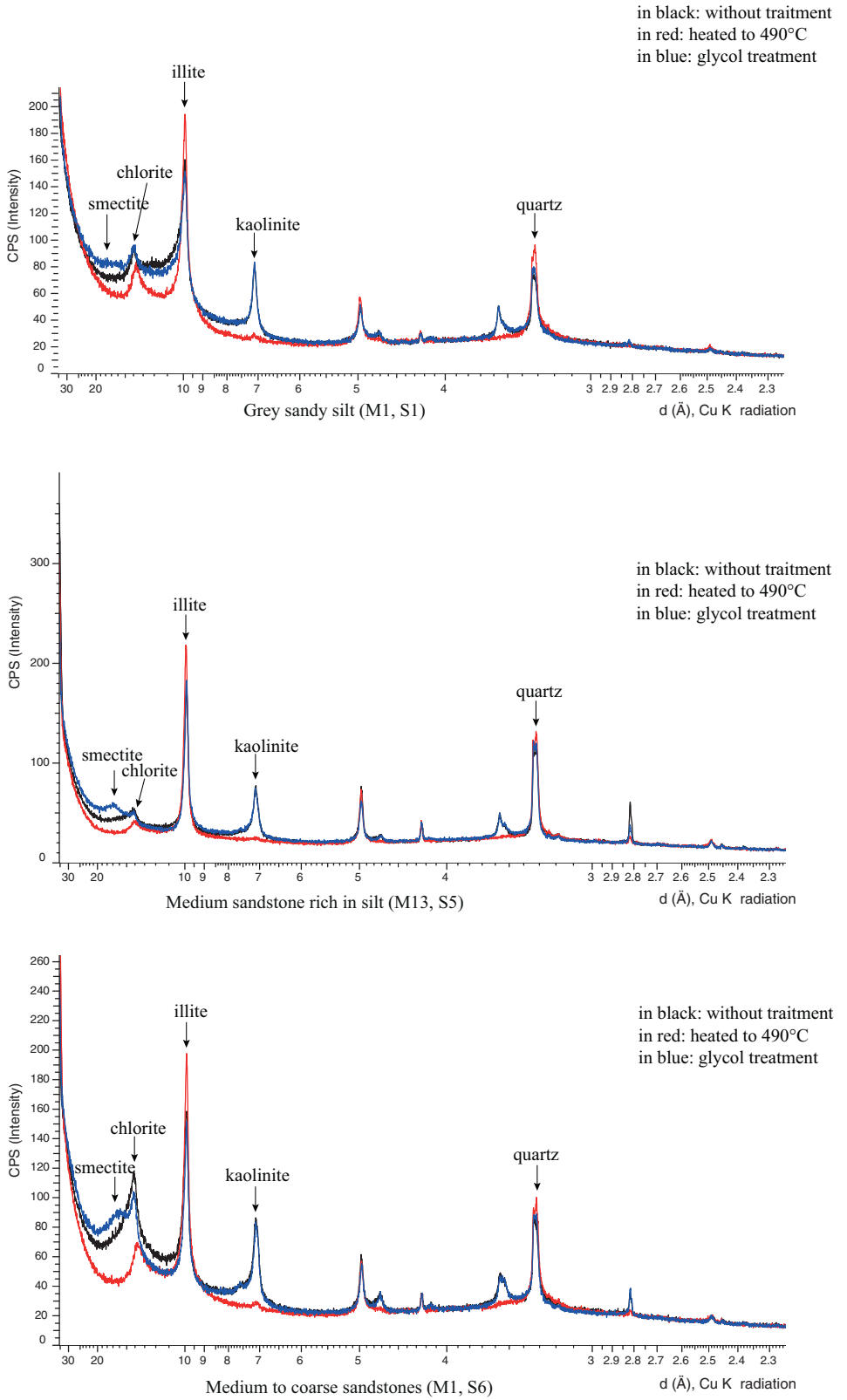

Fig. 8. X-Ray Diffractogram for clay mineralogy of some representative samples. On the *Y*-axis: CPS: counts per second. On the *X* axis, *d*: angular values (in ångströms). In order to show the XRD pattern, the interplanar spacing *d* on the *X* axis is partly on logarithmic scale and partly on linear scale.
Fig. 8. Diffractogramme RX des argiles de quelques échantillons représentatifs. Sur l'axe *Y* : CPS : coups par seconde. Sur l'axe *X*, *d* : valeurs angulaires (en ångströms). Pour représenter toute la gamme des valeurs, l'axe *X* est en partie en échelle logarithmique et en partie en échelle linéaire.

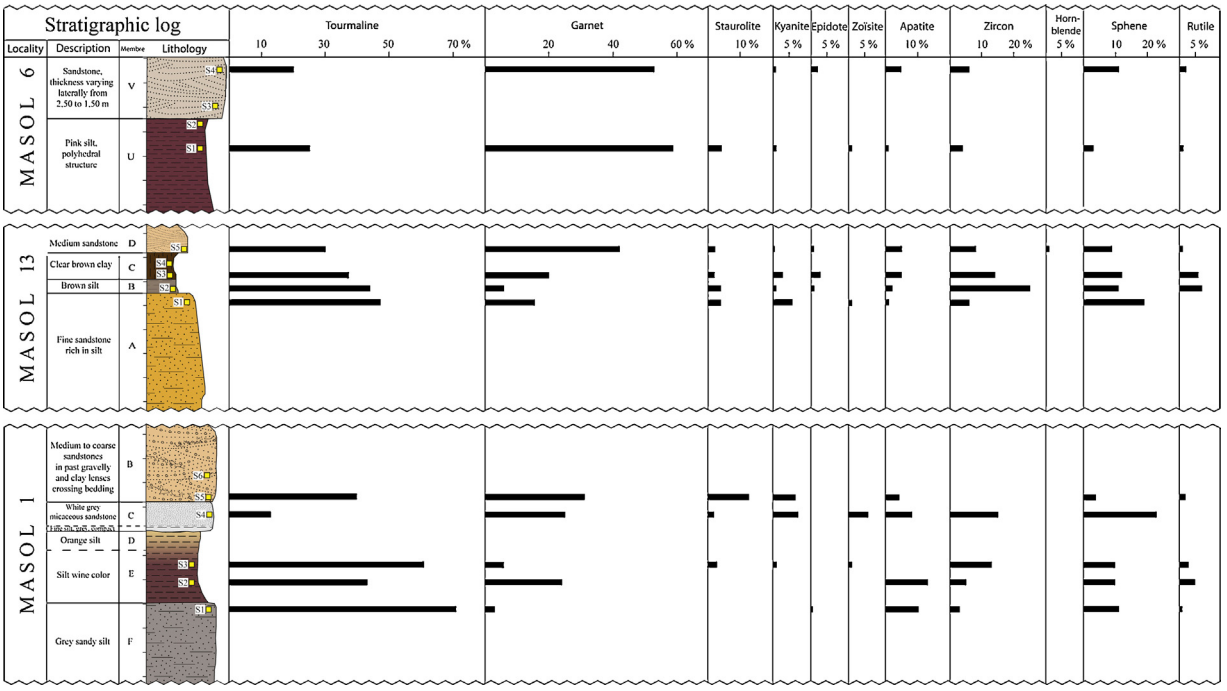

Fig. 9. Diagram of the results of heavy minerals of Masol 1, Masol 13 and Masol 6.
Fig. 9. Diagramme des résultats pour les minéraux lourds de Masol 1, Masol 13 et Masol 6.

- An intense peak (D1) is seen at 10.1 Å due to the illite (Fig. 8). Such a peak at 5.00 Å suggests that the mineral (illite) is in its hydrated form.
- The kaolinite is also abundant in all the localities except in the micaceous fine sandstone (member C), and in the gray sandy silt (member F) of Masol 1.
- The chlorite is not homogeneously distributed in all the sedimentological layers. The spectral shape of the chlorite peak in the spectra suggests that the crystalline network is not very developed.
- The smectite is seen with a heterogeneous distribution in the various layers, its peak is well defined at 12 Å only after using glycol.

4.3. *Heavy minerals*

Masol 1 paleonto-archeological locality

Tourmaline represents 40 to 71% of the heavy minerals. It is the most abundant mineral in all the samples. There is only one sample (S4, in the micaceous fine sandstone member) where garnet (25%) reaches values comparable to tourmaline (25%). The average abundance of sphene is 12%; it varies from 4% (in the medium to coarse sand member "B", S5) to 23% (in the micaceous sandstone member C, S4). Apatite proportions range between 1 and 13% (average 8%) and zircon between 3 and 15% (average 7%). The other detected minerals are the staurolite (4%), the kyanite (3%) and the rutile (2%) (Fig. 9).

Silt members contain the highest amounts of tourmaline and apatite. Sandstone and sandy Members B and C contain much garnet, sphene, staurolite, kyanite and zircon (Fig. 9).

Masol 13 paleonto-archeological locality

Tourmaline abundance ranges between 31 and 47%. There is a decrease from the bottom to the top of the section. The proportion of garnet ranges between 42% in the medium sandstone (member D) (S5) and 6% in the brown silt (member B) (S2). Zircon abundance in this silt (S2) is 25%, 14% in clay (S3), 6% in fine sandstone (S1) and 8% in medium sandstone (S5). The zircon abundance decreases from the bottom to the top of the section. Sphene has a higher content in the sandstone (S1) (19%) than in the sandstone (S5) (9%) and remains constant at 12% in silt (S2) and clay (S3). Kyanite reaches 6% in S1 and is rare in S5. Staurolite abundance ranges between 4% in the lower part of the sequence (S1), and 2% in its upper part (S5; Fig. 9). Rutile shows higher rates in silt "S2" and clay "S3" (respectively 7% and 6%) than in sandstones (S5 with 1%). Epidote abundance is constant in S2 and S5 (1%) and reaches a slightly higher percentage (3%) in S5 (Fig. 9).

Tourmaline, sphene, zircon, rutile and staurolite decrease from the bottom (S1, Fig. 9) to the top (S5) of the locality. Conversely, garnet abundance increases from the bottom to the top of the locality.

Masol 6 paleonto-archeological locality

This locality is characterized by a significant abundance of garnet (56%) and a relative decrease in tourmaline (22%) in comparison to Masol 1 and Masol 13 (Fig. 9). The silt layer with a polyhedral structure "U" contains more staurolite, while the sandstone member "V" contains more sphene, zircon and apatite (Fig. 9).

Heavy mineral synthesis

Tourmaline and garnet constitute the most significant proportions in the mineralogical assemblage of Masol (> 66%). These two minerals indicate opposite evolutions. In sandstone members, the proportion of tourmaline decreases significantly and the garnet increases. In the silty and clay members, tourmaline represents more than half the mineralogical assemblage. Sphene and zircon average rates are similar. Sphene has a constant occurrence in all the layers. Zircon abundance is higher in the silt and clay members. Apatite proportions are higher in layers where grain sizes are smaller. Staurolite and kyanite frequencies are slightly higher in the sand and the sandstone layers than in the silty members. Epidote is absent from Masol 1. The highest proportions of rutile are observable in the silt and clay members.

Mica (muscovite and biotite) rates range from 4 to 90%. A rate of 90% is reached in medium to coarse sand member "B" in Masol 1. When considered, this abundance hides the relative proportion between the other minerals. We have therefore excluded the micas from the counting. Tourmaline is usually brown and subangular (only one grain is blue). Garnet is often altered. Many minerals demonstrate no marks of erosion. The mineralogical assemblage composition suggests a metamorphic source.

5. Discussion of the geological and geographical origins of the minerals

5.1. Mineralogical content: synthesis

Singh et al. (2004) studied the mineralogical assemblage of the Cenozoic sequences in the Jammu region (Northwest Himalaya), the sediments of the Murree Group (Early Miocene of Northwest Indian subcontinent) (Fig. 10A), the sand of the Baspa River which originate in the Higher Himalaya before joining the Sutlej River at Karcham (Fig. 10B), and the sand of the Bhuzas stream flowing in the Lesser Himalaya before joining the Chenab river at Atholi (Fig. 10C). The Bhuzas stream that flows from north-east to south-west crosses the main metamorphic formations before reaching the Chenab River. These metamorphic formations are gneiss and schist with veins of quartz, granites, amphibolites and pegmatites. The mineralogical assemblage contains sillimanite, garnet, kyanite, staurolite and biotite-mica.

The Baspa River, a tributary of the Sutlej, is generally oriented east-west before diverging to the north at Sangla. The Baspa successively crosses phyllitic formations, quartzite and granite, gneiss with psammites, porphyroblastic gneiss and schists, and in its downstream portion, granitic formations. The minerals contained in theses formations are garnet, kyanite, sillimanite and biotite-mica (Singh et al., 2004).

Table 1 allows a comparison of the mineralogical compositions of a) the rivers Baspa and Bhuzas, b) the Jammu region, c) the Murree Group, d) the Siwalik Group, and e) the localities of Masol. The studies of Singh et al. (2004) show the constant presence of garnet, tourmaline, epidote, staurolite, zircon and kyanite for a), b) c) and d). Hornblende is seen in the sand formation in the Jammu region, and sillimanite is absent from the Murree Group. Another interesting point is the absence of sphene, apatite and rutile in the rivers, but also in the Jammu region and the Murree Group. Sphene is also absent in Lower and Middle Siwalik, and apatite and rutile are absent in Siwalik group

The Siwalik deposits contain ten species of heavy minerals (Delcaillau, 1986; Raju and Dehadrai, 1962). Garnet, tourmaline, epidote, staurolite, zircon and zoïsite are common to the three subgroups of the Lower, Middle and Upper Siwalik. Kyanite is absent in the Lower Siwalik (where it should have an exceptional presence according to Delcaillau) while hornblende, sillimanite, andalusite and sphene are present only in the Upper Siwalik. The Lower and the Middle Siwalik differ from the Upper Siwalik in the absence of several minerals such as the hornblende, the sillimanite, the andalusite and the sphene.

The comparison of the mineralogical assemblages of the various sites with these of the paleonto-archeological localities of Masol shows that this sequence from Masol contains the richest assemblage of minerals. They differ in the absence of sillimanite and the presence of apatite and rutile. The diversity of the mineralogical content is due to the various geological formations drained by the different rivers, and to the heterogeneous resistance of minerals to the transport processes. These observations are consistent with the recent conclusions of Dubille and Lavé (2015), despite the dissimilarity in the mineralogical content, however, the entire Upper Siwalik subgroup (Masol localities included) contains generally the same heavy minerals.

5.2. Clay mineral content and sedimentation context

The minerals identified in the Masol Formation contain illite, kaolinite, chlorite and smectite as previously seen in the Late Neogene sediments of the Subathu subbasin and in the Siwalik by Suresh et al. (2004) and Delcaillau (1986), respectively. Sediment deposits and mineral content could be influenced by (i) rock mineral initial content, (ii) climate, (iii) topography, (iv) diagenesis and (v) transport dynamic.

(i) Rock mineral initial content: both illite and chlorite are produced by the physical alteration or transformation of crystalline rocks (Ghosh et al., 2003; Kumar et al., 1999). Kaolinite results from magmatic rocks and smectite originates from the magmatic or volcanic rocks of the Lesser Himalayan hinterland (Raiverman and Suresh, 1997). In conclusion, the minerals seen in the three localities of the Masol Formation have been transported (1) from the crystalline rocks of the Higher Himalaya, composed of orthogneiss (magmatic) and paragneiss (metamorphic), and (2) from the volcanic and sedimentary rocks of the Lesser Himalaya.

(ii) Climate: various studies suggest that illite and chlorite are formed during cold and dry climate, while smectite and kaolinite occur during hot and wet climates (Chamley, 1989; Gibson et al., 2000). The alternation of these minerals could suggest climatic variations in their source area.

(iii) Topography: the presence of the kaolinite throughout the stratigraphic sequences of the three localities of Masol is due to a stable environment. Smectite was

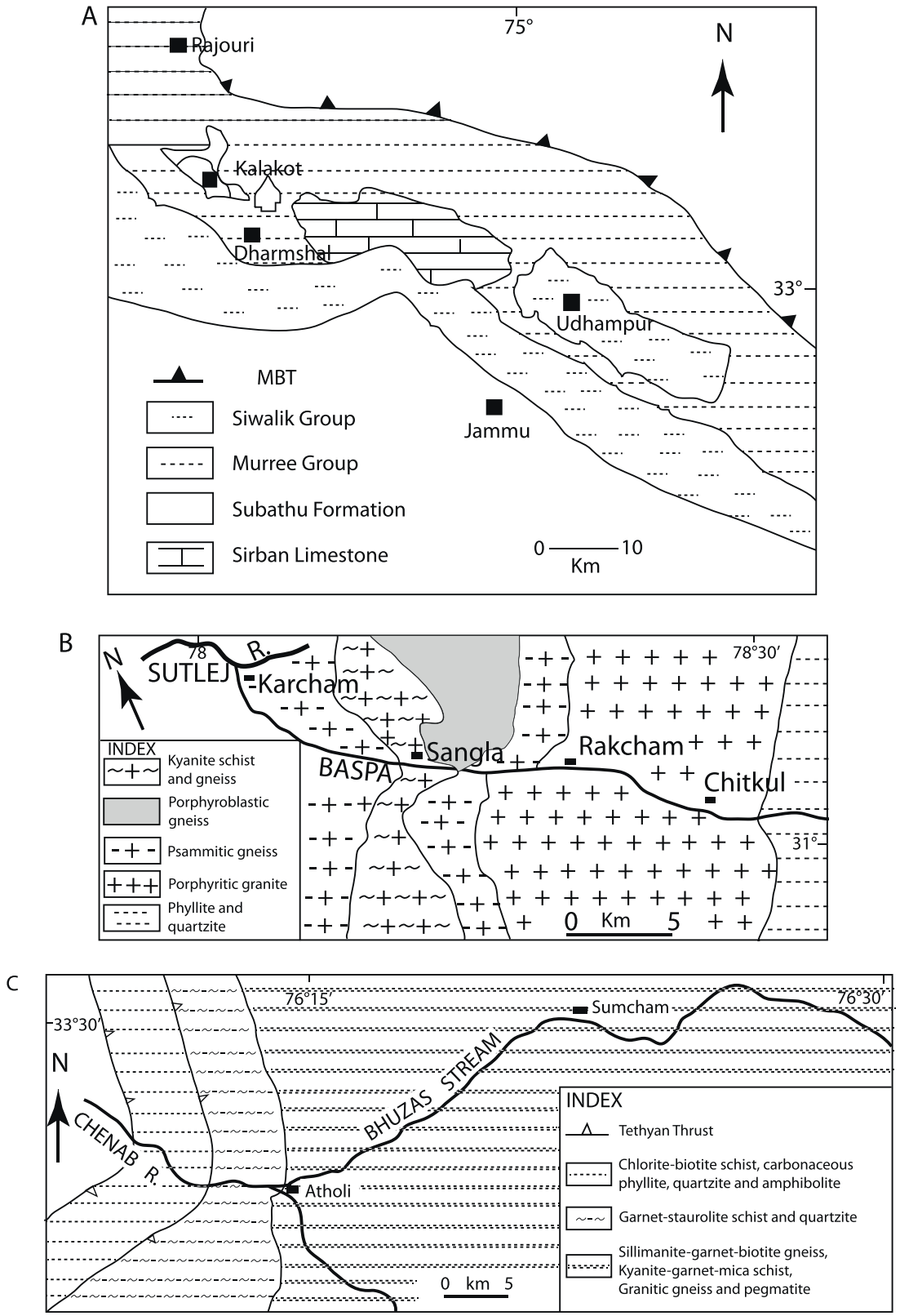

Fig. 10. (A) Geological map of the Cenozoïc belt of the Jammu area; B: geological map showing disposition of various rock types in the Baspa Valley; C: geological map exhibiting different rock units in the Bhuzas Valley (Singh et al., 2004).
Fig. 10. (A) Carte géologique de la ceinture cénozoïque de la zone de Jammu ; (B) carte géologique montrant la disposition des divers types de roches dans la vallée de la Baspa ; (C) carte géologique présentant les différentes unités lithologiques dans la vallée de Bhuzas (Singh et al., 2004).

Table 1
Comparison of the mineralogical assemblages of sediments resulting from rivers of Baspa and Bhuzas, deposits from Jammu, Murree Group, Siwalik Group and the three localities of Masol, M1, M6, M13.
Tableau 1
Comparaison des cortèges minéralogiques des sédiments provenant des rivières Baspa et Bhuzas, des dépôts du Jammu, du groupe Murree, du groupe Siwalik et des trois localités de Masol, M1, M6, M13.

Minerals	Baspa	Bhuzas	Jammu	Murree Groupe	Lower Siwalik	Middle Siwalik	Upper Siwalik	Masol 1	Masol 6	Masol 13
Garnet	+	+	+	+	+	+	+	+	+	+
Tourmaline	+	+	+	+	+	+	+	+	+	+
Epidote	+	+	+	+	+	+	+	+	+	+
Staurolite	+	+	+	+	+	+	+	+	+	+
Zircon	+	+	+	+	+	+	+	+	+	+
Zoïsite					+	+	+	+	+	+
Kyanite	+	+	+	+		+	+	+	+	+
Hornblende			+				+			+
Sillimanite	+	+	+				+			
Andalusite							+	+	+	
Sphene							+	+	+	+
Apatite								+	+	+
Rutile								+	+	+

identified in members with fine textures such as silt, clay or micaceous fine sandstone. This suggests a low energy deposit environment such as in a floodplain.

(iv) Diagenesis: smectite is less abundant in coarser sandstone, whereas illite abundance increases: this could be due to a diagenetic modification of the smectite after dewatering (Keller, 1970); however, the absence of any trend in the mineralogical content argues against the effects of a strong diagenesis in the transformation of the clay minerals.

(v) Transport dynamic: the significant quantity of weak minerals, such as apatite, in the sediment deposits suggests a moderate transport from the Himalayas to the foothills or/and a protective transport process, such as a mud flow. In a second phase, those sediments were deposited in the floodplains by relatively low energy river flows (the presence of silt and fine sand with seasonal contrasts which is certainly enhanced by the monsoon as evidenced by coarse sand and pebbles). The chlorite/illite association is generally dominant. Its relative decrease in silt members in comparison with smectite/kaolinite mineralogical content could be due to variation of the river flow energy.

6. Conclusions

The mineralogical composition of sediments from Masol localities (Masol 1, 6 and 13) indicates that the sediments originated from the Higher and Lesser Himalaya. There is no significant diagenesis seen. The nature and the appearance of the detrital particles (not rounded, not altered) suggest that the material was transported by mud flows (moderate energy river), and then deposited in alluvial fans in the floodplain bordering the foothills. The gentle slope of the Indo-Gangetic plain allowed a decrease of the river flow energy and favored finer sediment deposits. This flat surface, comprised of fluvial deposits, was then deformed when the Himalayan Frontal Fault began uplifting the Siwalik Range. The particle size distribution and the sedimentological variations could be due to river flow changes related to the monsoon seasonal activity, however, autocyclic morphological evolution (slope, distance) of the streams flowing in the frontal range cannot be excluded. Gravels, quartzite and pebbles seen in the field probably correspond to ancient accretion bars.

Acknowledgments

The Indo-French program of research “Siwaliks” is under the patronage of Professor Yves Coppens, College of France and Academy of Sciences, Institute of France since 2012 with the financial support of the French Ministry of Foreign Affairs (2012–2014), and the financial support of the National Museum of Natural History, a) the Department of Prehistory (2007, 2010, 2011) and b) the ATM grant of the Department of Earth Sciences (2011). We are thankful to the Archaeological Survey of India and to the Department of Tourism, Cultural Affairs, Archaeology and Museums of Punjab Government for survey permit. We are grateful to the Sarpanch of Masol village, for his hospitality. We thank Pr. Piotr Tucholka, University Paris-Sud, for his suggestions and constructive remarks.

References

Anderson, J.R., 2007. Sand sieve Analysis. In: Gore, P.J.W. (Ed.), Historical Geology Online Laboratory Manual. Department of Geology, Georgia Perimeter College, 278 p.

Badam, G.L., 1973. Geology and palaeontology of the Upper Siwaliks of a part of Pinjore-Nalagarh area. Faculty of Science and Mathematics, Panjab University, Chandigarh (Ph.D. Thesis), 185 p.

Caillère, S., Hénin, S., Rautureau, M., 1982. Minéralogie des argiles. 1. Structures et propriétés physico-chimiques. INRA, Actualités scientifiques et agronomiques, 8., 2e éd. Masson, Paris, 184 p.

Chamley, H., 1989. Clay Sedimentology. Springer-Verlag, New York, 623 p.

Chapon Sao, C., Abdessadok, S., Tudryn, A., Dambricourt Malassé, A., Singh, M., Karir, B., Gaillard, C., Moigne, A.M., Gargani, J., Bhardwaj, V., 2016a. Lithostratigraphy of Masol paleonto-archeological localities in the Quranwala Zone, 2.6 Ma, northwestern India. In Human origins on the Indian sub-continent. C. R. Palevol 15 (this issue).

Chapon Sao, C., Abdessadok, S., Dambricourt Malassé, A., Singh, M., Karir, B., Bhardhwaj, V., Pal, S., Gaillard, C., Moigne, A.M., Gargani, J., Tudryn, A., 2016b. Magnetic polarity of Masol 1 Locality deposits, Siwalik Frontal Range, northwestern India. In Human origins on the Indian sub-continent. C. R. Palevol 15 (this issue).

Dambricourt Malassé, A., 2016. The first Indo-French Prehistorical Mission in Siwaliks and the discovery of anthropic activities at 2.6 million years. In Human origins on the Indian sub-continent. C. R. Palevol 15 (this issue).

Dambricourt Malassé, A., Singh, M., Karir, B., Gaillard, C., Bhardwaj, V., Moigne, A.M., Abdessadok, S., Chapon Sao, C., Gargani, J., Tudryn, A., Calligaro, T., Kaur, A., Pal, S., Hazarika, M., 2016a. Anthropic activities in the fossiliferous Quranwala Zone, 2.6 Ma, Siwaliks of Northwest India, historical context of the discovery and scientific investigations. In Human origins on the Indian sub-continent. C. R. Palevol 15 (this issue).

Dambricourt Malassé, A., Moigne, A.M., Singh, M., Calligaro, T., Karir, B., Gaillard, C., Kaur, A., Bhardwaj, V., Pal, S., Abdessadok, S., Chapon Sao, C., Gargani, J., Tudryn, A., Garcia Sanz, M., 2016b. Intentional cutmarks on bovid from the Quranwala Zone, 2.6 Ma, Siwalik Frontal Range, NW India. In Human origins on the Indian sub-continent. C. R. Palevol 15 (this issue).

DeCelles, P.G., Gehrels, G.E., Quade, J., Ojha, T.P., Kapp, P.A., Upreti, B.N., 1998. Neogene foreland basin deposits, erosional unroofing, and the kinematic history of the Himalayan fold-thrust belt, western Nepal. Geol. Soc. Am. Bull. 110, 2–21.

Delcaillau, B., 1986. Evolution géomorphostructurale d'un piémont frontal de chaîne de collision intracontinentale : les Siwaliks de l'Himalaya du Népal oriental. Institut de Géographie Daniel Faucher, Université de Toulouse, Thèse, 435 p.

Dunoyer de Segonzac, G., Ferrero, J., Kubler, B., 1968. Sur la cristallinité de l'illite dans la diagenèse et l'anchimétamorphisme. Sedimentology 10 (2), 137–143.

Dubille, M., Lavé, J., 2015. Rapid grain size coarsening at sandstone/conglomerate transition: similar expression in Himalayan modern rivers and Pliocene molasse deposits. Basin Res. 27 (1), 26–42.

Duplaix, S., 1958. Détermination microscopique des minéraux des sables. Librairie Polytechnique Ch. Béranger, Paris et Liège, 96 p.

Folk, P.L., Ward, W.C., 1957. Brazos river bar: a study in the significance of grain size parameters. J. Sediment. Petrol. 27, 3–26.

Gaillard, C., Singh, M., Dambricourt Malassé, A., Bhardwaj, V., Karir, B., Kaur, A., Pal, S., Moigne, A.M., Sao Chapon, C., Abdessadok, S., Gargani, J., Tudryn, A., 2016. The lithic industries on the fossiliferous outcrops of the Late Pliocene Masol Formation, Siwalik Frontal Range, northwestern India (Punjab). In Human origins on the Indian sub-continent. C. R. Palevol 15 (this issue).

Gargani, J., Abdessadok, S., Tudryn, A., Chapon Sao, C., Dambricourt Malassé, A., Gaillard, C., Moigne, A.M., Singh, M., Bhardwaj, V., Karir, B., 2016. Geology and geomorphology of Masol paleonto-archeological site, Late Pliocene, Chandigarh anticline, Siwalik Frontal Range, NW India. In Human origins on the Indian sub-continent. C. R. Palevol 15 (this issue).

Gaur, R., 1987. Environment and ecology of early Man in Northwest India. B. R. Publishing Corporation, Delhi.

Ghosh, S.K., Kumar, R., Suresh, N., 2003. Influence of Mio-Pliocene drainage reorganisation in the detrital modes of sandstone, Subathu sub-basin. Himalayan foreland basin. J. Him. Geol. 24, 35–46.

Gibson, T.G., Bybell, L.M., Mason, D.B., 2000. Stratigraphic and climatic implications of clay mineral changes around the Paleocene/Eocene boundary of the northeastern US margin. Sediment. Geol. 134, 65–92.

Holtzapffel, T., 1985. Les minéraux argileux. Préparation, Analyse diffractométrique et détermination. Société Géologique du Nord, Publication 12, 136 p.

Jangpangi, B.S., Dhaundiyal, D.P., Kumar, G., Dhaundiyal, J.N., 1978. On the geology of Sumcham sapphire mines area, Doda district, Jammu and Kashmir. Him. Geol. 8 (2), 837–849.

Keller, W.D., 1970. Environmental aspects of clay minerals. J. Sediment. Petrol. 40, 785–813.

Kumar, R., Ghosh, S.K., Sangode, S.J., Padtare, N.R., 1999. Evolution of the Plio-Pleistocene contrasting alluvial fans in the Siwalik foreland basin, NW Himalaya, India. Gondwana Res. Group Mem. 6, 295–304.

Larqué, P., 2002. Diffractométrie de la minéralogie de la fraction argileuse. In: Miskovsky, J.C. (Ed.), Géologie de la Préhistoire : méthodes, techniques, applications. Éd. Association pour l'étude de l'environnement géologique de la préhistoire (GEOPRE), Paris, pp. 601–613.

Lucas, J., Camez, T., Millot, G., 1959. Détermination pratique aux rayons X des minéraux argileux simples et interstratifiés. Bull. Serv. Carte Geol. Als. Lorr. 12, 21–23.

2000. Manuel du granulomètre Laser Mastersizer.

Millot, G., 1964. Géologie des argiles. Masson, Paris, 499 p.

Miskovsky, J.C., Debard,.E., 2002. Granulométrie des sédiments et étude de leur fraction grossière. In: Miskovsky, J.C. (Ed.), Géologie de la Préhistoire : méthodes, techniques, applications. Éd. Association pour l'étude de l'environnement géologique de la préhistoire (GEOPRE), Paris, pp. 480–501.

Moigne, A.M., Dambricourt Malassé, A., Singh, M., Bhardwaj, V., Gaillard, C., Kaur, A., Karir, B., Pal, S., Abdessadok, S., Chapon Sao, C., Gargani, J., Tudryn, A., 2016. The faunal assemblage of the paleonto-archeological localities of Masol Formation, Late Pliocene Quranwala Zone, NW India. In Human origins on the Indian sub-continent. C. R. Palevol 15 (this issue).

Nanda, A.C., 1994. Upper Siwalik mammalian faunas from Chandigarh and Jammu regions with comments on certain faunal discrepancies. In: Ahmed, A., Sheikh, A.M. (Eds.), Geology in South Asia-1. Hydrocarbon Institute of Pakistan, Islamabad, pp. 39–45.

Parfenoff, A., Pomerol, Ch., Tourenq, J., 1970. Les minéraux en grains. Méthodes d'étude et détermination. Masson, 578 p.

Patnaik, R., 2013. Indian Neogene Siwalik mammalian biogeography, Chap 17. In: Wang, X., Flynn, L.J., Fortelius, M. (Eds.), Fossil mammals of Asia Neogene biostratigraphy and chronology. Columbia University Press, New York, pp. 423–444.

Pédro, G., 1965. La classification des minéraux argileux (Phyllosilicates). Étude historique et considérations critiques. Institut National de la Recherche Agronomique, Annales agronomiques 6, hors-série, 1, 108 p.

Petitjohn, F.J., 1975. Sedimentary Rocks, Third ed. Harper and Bros, New York.

Pye, K., Blott, J.S., 2004. Particle size analysis of sediments, soils and related particulate materials for forensic purposes using laser granulometry. Forensic Sci. Int. 144 (1), 19–27.

Raiverman, V., Suresh, N., 1997. Clay mineral distribution in the Cenozoic sequence of the western Himalayan Foothills. J. Indian Assoc. Sediment. 16, 63–75.

Raju, A.T.R., Dehadrai, P.V., 1962. Note on heavy mineral classification of Siwalik sediments from Jammu and the Panjab. Curr. Sci. 31, 378 p.

Ranga Rao, A., 1993. Magnetic-polarity stratigraphy of Upper Siwalik of north-western Himalayan foothills. Curr. Sci. 64 (11–12), 863–873.

Ranga Rao, A., Nanda, A.C., Sharma, U.N., Bhalla, M.S., 1995. Magnetic polarity stratigraphy of the Pinjor Formation (Upper Siwalik) near Ninjore, Haryana. Curr. Sci. 68 (12), 1231–1236.

Rivière, A., 1977. Méthodes granulométriques. Techniques et interprétations. Coll. Techniques et méthodes granulométriques. Masson édition, Paris, 170 p.

Robert, M., 1975. Principes de détermination qualitative des minéraux argileux à l'aide de rayons X. Annales Agronom. 26 (4), 363–399.

Sahni, M.R., Khan, E.J., 1968. Stratigraphy, structure and correlation of the Upper Shiwaliks, East of Chandigarh. J. Palaeontol. Soc. India 19601964 (59), 61–74.

Singh, B.P., Pawar, J.S., Karlupia, S.K., 2004. Dense mineral data from the northwestern Himalayan foreland sedimentary rocks and recent river sediments: evaluation of the hinterland. J. Asian Earth Sci. 23, 25–35.

Suresh, N., Ghosh, S.K., Rohtash, K., Sangode, S.J., 2004. Clay-mineral distribution patterns in Late Neogene fluvial sediments of the Subathu sub-basin, central sector of Himalayan foreland basin: implications for provenance and climate. Sediment. Geol. 163, 265–278.

Tandon, S.K., 1972. Heavy minerals and quartz axial ratios as provenance indicators in the Siwalik sediments around Ramnagar, Kumaun Himalaya. Himalayan Geo. 3, 206–221.

Thakur, V.C., Rawat, B.S., Islam, R., 1990. Zanskar Crystalline, some observations on its lithostratigraphy, deformation, metamorphism and regional framework. Jour. Him. Geol. 1, 11–25.

Tourenq, J., 2002. Minéraux lourds. In: Miskovsky, J.C. (Ed.), Géologie de la Préhistoire : méthodes, techniques, applications. Éd. Association pour l'étude de l'environnement géologique de la préhistoire (GEOPRE), Paris, pp. 555–569.

Tudryn, A., Abdessadok, S., Gargani, J., Dambricourt Malassé, A., Singh, M., Gaillard, C., Bhardwaj, V., Chapon Sao, C., Moigne, A.M., Karir, B., Pal, S., Miska, S., 2016. Stratigraphy and paleoenvironment during the Late Pliocene at Masol paleonto-archeological site (Siwalik Range, NW India): preliminary results. In Human origins on the Indian sub-continent. C. R. Palevol 15 (this issue).

Warwick, P.D., 2007. Overview of the geography, geology and structure of the Potwar regional framework assessment project study area, northern Pakistan. In: Warwick, P.D., Wardlaw, B.R. (Eds.), Regional Studies of the Potwar Plateau Area, northern Pakistan. US Geol. Surv. Bull., p. 2078.